

Vector and Axial-Vector Mesons in Nuclear Matter

Ralf-Arno Tripolt^{1,2}

in collaboration with

Tetyana Galatyuk^{2,3,4}, Lorenz von Smekal^{1,2}, Jochen Wambach³, Maximilian Wiest^{3,4}

¹JLU Giessen, ²HFHF, ³TU Darmstadt, ⁴GSI



Hard Probes 2023, Aschaffenburg, March 30, 2023



I) Introduction and motivation

- ▶ heavy-ion collisions, QCD phase diagram, dileptons

II) Theoretical setup

- ▶ Functional Renormalization Group
- ▶ parity-doublet model
- ▶ spectral functions with the aFRG method

III) Results on spectral functions and dileptons

- ▶ in-medium ρ and a_1 spectral functions
- ▶ thermal dilepton rates and spectra

IV) Summary and outlook

Introduction and motivation

QCD phase diagram

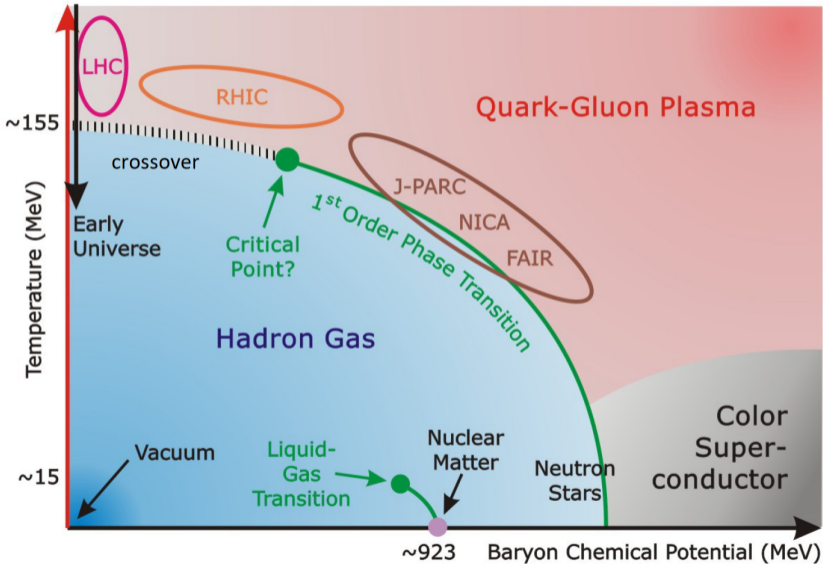


[Figure adapted from the CRC-TR 211 funding proposal]

Dileptons in heavy-ion collisions

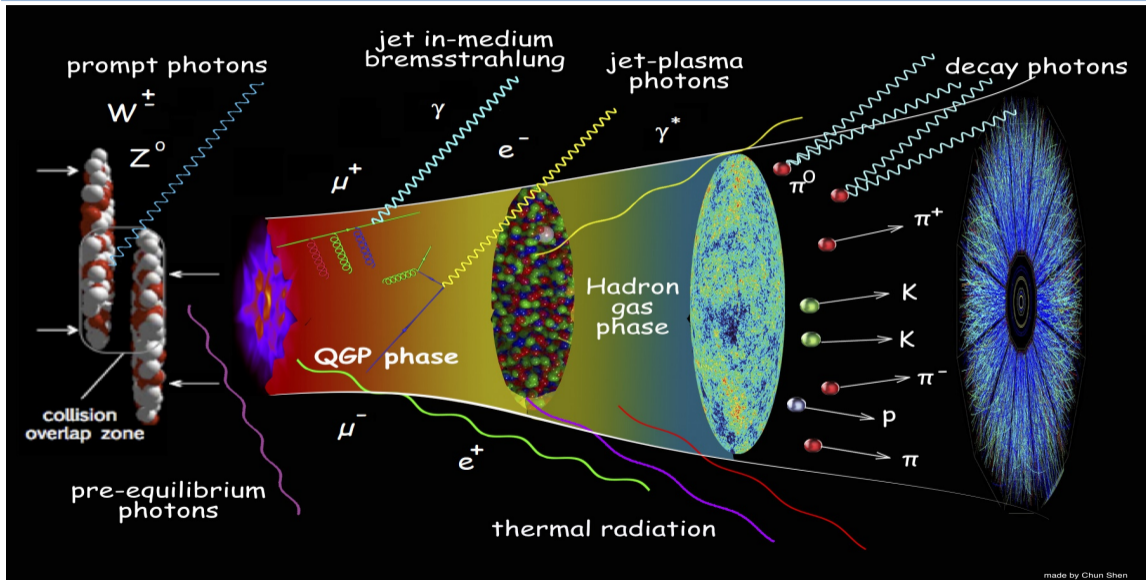
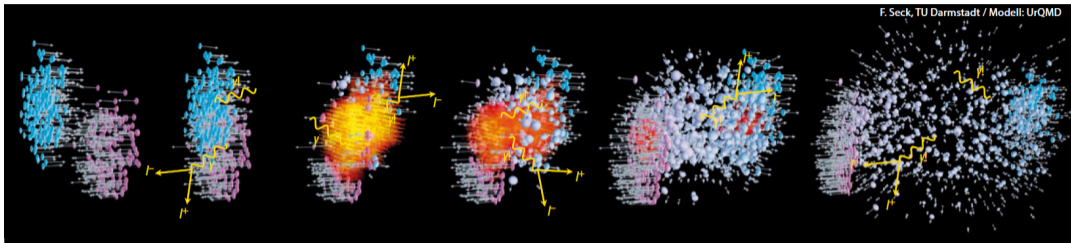


[Figure by Chun Shen]

Why dileptons?

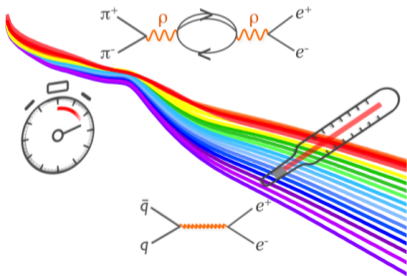


- ▶ Electromagnetic (EM) probes, i.e. photons and dileptons, don't interact 'strongly' with medium
 - ▶ they have a long mean free path and can carry information from production site to detectors
 - ▶ they are produced at all stages of the collision
- **dileptons are uniquely well-suited to study hot and dense matter in heavy-ion collisions!**

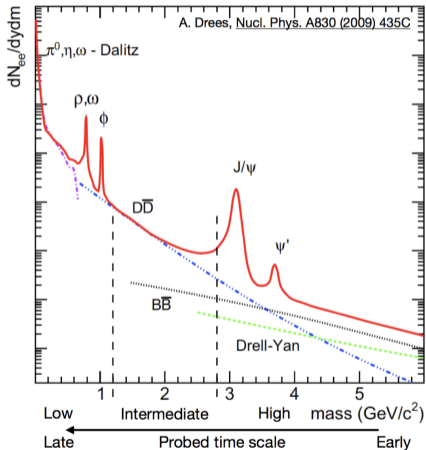
What can we learn from dileptons?

Dileptons contain information on:

- ▶ temperature, fireball lifetime, in-medium spectral functions, chiral symmetry, changes in degrees of freedom, transport coefficients (electrical conductivity), ...



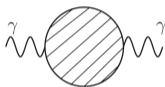
[T. Galatyuk, H. v. Hees, R. Rapp, J. Wambach, Physik Journal 17, Nr. 10 (2018)]



Dilepton production rates

Thermal field theory: Electromagnetic correlation function

$$\Pi_{\text{EM}}^{\mu\nu}(M, p; \mu_B, T) = -i \int d^4x e^{ip \cdot x} \Theta(x_0) \langle\langle [j_{\text{EM}}^\mu(x), j_{\text{EM}}^\nu(0)] \rangle\rangle$$



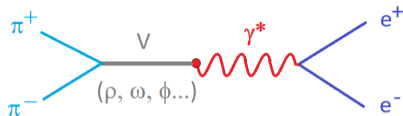
determines both **photon and dilepton rates**:

▶ photons:
$$p_0 \frac{dN_\gamma}{d^4x d^3p} = -\frac{\alpha_{\text{EM}}}{\pi^2} f^B(p_0; T) \frac{1}{2} g_{\mu\nu} \text{Im} \Pi_{\text{EM}}^{\mu\nu}(M=0, p; \mu_B, T),$$

▶ dileptons:
$$\frac{dN_{ll}}{d^4x d^4p} = -\frac{\alpha_{\text{EM}}^2}{\pi^3 M^2} L(M) f^B(p_0; T) \frac{1}{3} g_{\mu\nu} \text{Im} \Pi_{\text{EM}}^{\mu\nu}(M, p; \mu_B, T),$$

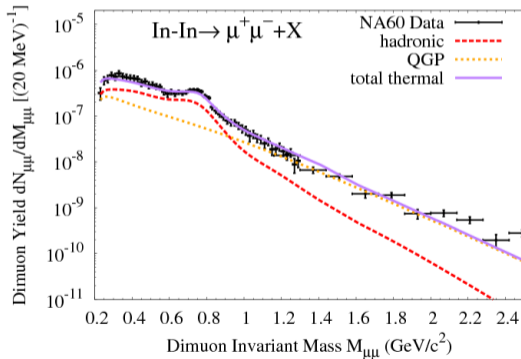
Connection between dileptons and vector mesons

Vector mesons have the same quantum numbers as photons and can decay directly into dileptons:



Excess dimuon invariant-mass spectrum as measured in In-In collisions at $\sqrt{s_{NN}} = 17.3$ GeV by the NA60 collaboration at the SPS is well described by using **vector meson dominance**:

$$\text{Im}\Pi_{\text{EM}}^{\mu\nu}(M) \sim \text{Im}D_{\rho}^{\mu\nu} + \frac{1}{9}D_{\omega}^{\mu\nu} + \frac{2}{9}D_{\phi}^{\mu\nu}$$



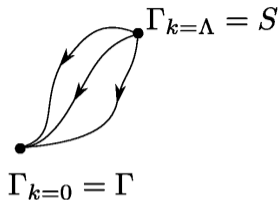
Theoretical setup

Method of choice: FRG

Functional Renormalization Group (FRG):

$$\partial_k \Gamma_k = \frac{1}{2} \text{STr} \left(\partial_k R_k \left[\Gamma_k^{(2)} + R_k \right]^{-1} \right)$$

[C. Wetterich, Phys.Lett. B301, 90 (1993)]



[wikipedia.org]

- ▶ non-perturbative continuum framework
- ▶ implements Wilson's coarse-graining idea: fluctuations integrated out
- ▶ Γ_k interpolates between bare action S in the UV and effective action Γ in the IR
- ▶ capable of describing phase transitions at finite temperature and density
- ▶ **analytically-continued FRG (aFRG) method gives access to spectral functions!**

Effective theory for nuclear matter

We use the **parity-doublet model** with $N_1 = N(938) = (n, p)$, $N_2 = N^*(1535)$:

$$\Gamma_k = \int d^4x \left\{ \bar{N}_1 (\not{\partial} - \mu_B \gamma_0 + h_1(\sigma + i\vec{\tau} \cdot \vec{\pi} \gamma^5)) N_1 + \bar{N}_2 (\not{\partial} - \mu_B \gamma_0 + h_2(\sigma - i\vec{\tau} \cdot \vec{\pi} \gamma^5)) N_2 \right. \\ \left. + m_{0,N} (\bar{N}_1 \gamma^5 N_2 - \bar{N}_2 \gamma^5 N_1) + U_k(\phi^2) - c\sigma \right\}$$

- ▶ provides a phenomenologically successful description of nuclear matter
- ▶ describes **nuclear liquid-gas transition together with a chiral phase transition**
- ▶ accounts for a **finite nucleon mass** $m_{0,N}$ in a **chirally-invariant** fashion
- ▶ provides a natural description for the **parity-doubling structure** of the low-lying baryons

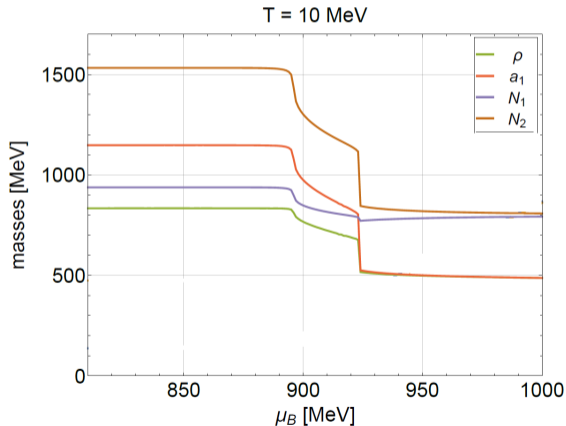
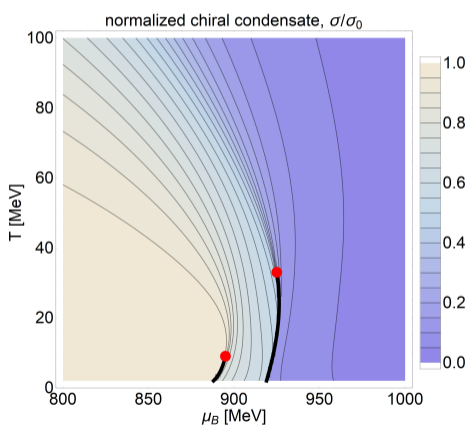
[C. E. Detar, T. Kunihiro, Phys. Rev. D 39, 2805 (1989)]

[R.-A. T., C. Jung, L. v. Smekal, J. Wambach, Phys. Rev. D 104, 054005 (2021)]

[F. Geurts, R.-A. T., Prog. Part. Nucl. Phys. 128, 104004 (2023)]

Parity-doublet model (I)

- describes nuclear liquid-gas transition together with a chiral phase transition:



Parity-doublet model (II)

Accounts for a **finite nucleon mass in a chirally-invariant fashion**:

- ▶ the **proton mass** can be obtained from the trace of the energy-momentum tensor of QCD

$$T \equiv T_{\mu}^{\mu} = \frac{\beta(g)}{2g} G^{\mu\nu a} G_{\mu\nu}^a + \sum_{l=u,d,s} m_l (1 + \gamma_{m_l}) \bar{q}_l q_l$$

$$\rightarrow \langle \mathbf{p}_1 | T | \mathbf{p}_2 \rangle \sim G(q^2), \quad G(0) = M$$

with the scalar gravitational form factor G

- ▶ only $\sim 8\%$ from chiral symmetry breaking ('sigma-term'), **rest from gluon term!**
- ▶ **mass radius of the proton** can be obtained as derivative w.r.t. momentum transfer $t = q^2$:

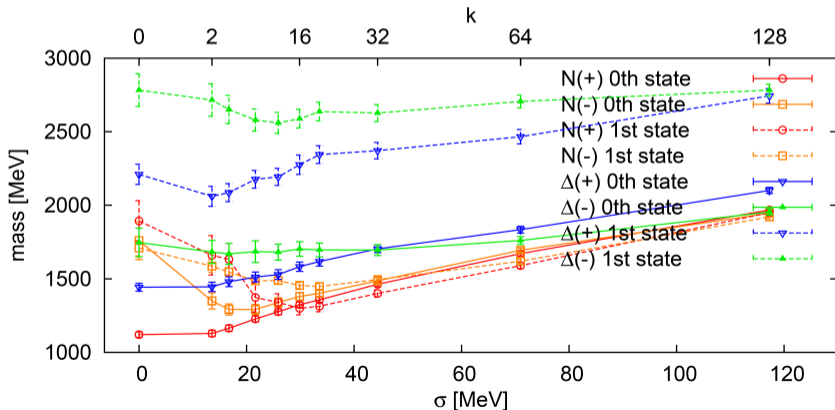
$$\langle R_m^2 \rangle = \frac{6}{M} \left. \frac{dG}{dt} \right|_{t=0}$$

\rightarrow GlueX data leads to $R_m \approx 0.55$ fm, as opposed to $R_c \approx 0.84$ fm!

Parity-doublet model (III)

Provides a natural description for the parity-doubling structure of the low-lying baryons:

- ▶ lattice simulations show **degeneration of parity partners** as chiral symmetry is (artificially) restored by removing the k lowest Dirac modes:



Introducing vector and axial-vector mesons

Parity-doublet model with vector mesons:

$$\begin{aligned}\Gamma_k = \int d^4x \left\{ \bar{N}_1 \left(\not{\partial} - \mu_B \gamma_0 + h_{s,1}(\sigma + i\vec{\tau} \cdot \vec{\pi} \gamma^5) + h_{v,1}(\gamma_\mu \vec{\tau} \cdot \vec{\rho}_\mu + \gamma_\mu \gamma^5 \vec{\tau} \cdot \vec{a}_{1,\mu}) \right) N_1 \right. \\ + \bar{N}_2 \left(\not{\partial} - \mu_B \gamma_0 + h_{s,2}(\sigma - i\vec{\tau} \cdot \vec{\pi} \gamma^5) + h_{v,2}(\gamma_\mu \vec{\tau} \cdot \vec{\rho}_\mu - \gamma_\mu \gamma^5 \vec{\tau} \cdot \vec{a}_{1,\mu}) \right) N_2 \\ + m_{0,N} \left(\bar{N}_1 \gamma^5 N_2 - \bar{N}_2 \gamma^5 N_1 \right) + U_k(\phi^2) - c\sigma + \frac{1}{2} (D_\mu \phi)^\dagger D_\mu \phi \\ \left. - \frac{1}{4} \text{tr} \partial_\mu \rho_{\mu\nu} \partial_\sigma \rho_{\sigma\nu} + \frac{m_v^2}{8} \text{tr} \rho_{\mu\nu} \rho_{\mu\nu} \right\}.\end{aligned}$$

- ▶ ρ and a_1 in terms of **anti-symmetric rank-2 tensor fields** which transform according to the (1,0) and (0,1) representations of the Euclidean O(4) group (with generators T_R and T_L):

$$\rho_{\mu\nu} = \rho_{\mu\nu}^+ + \rho_{\mu\nu}^- = \vec{\rho}_{\mu\nu}^+ \vec{T}_R + \vec{\rho}_{\mu\nu}^- \vec{T}_L$$

- ▶ the iso-triplet **vector and axial-vector fields** are obtained as

$$\vec{\rho}_\mu = \frac{1}{2m_v} \text{tr}(\partial_\sigma \rho_{\sigma\mu} \vec{T}_V), \quad \vec{a}_{1\mu} = \frac{1}{2m_v} \text{tr}(\partial_\sigma \rho_{\sigma\mu} \vec{T}_A)$$

Flow equations for ρ and a_1 2-point functions

$$\begin{aligned}
 \partial_k \Gamma_{\rho, k}^{(2)} = & \text{Diagram 1} + \text{Diagram 2} + \text{Diagram 3} - 2 \text{Diagram 4} - \frac{1}{2} \text{Diagram 5} \\
 \partial_k \Gamma_{a_1, k}^{(2)} = & \text{Diagram 6} + \text{Diagram 7} + \text{Diagram 8} + \text{Diagram 9} - 2 \text{Diagram 10} \\
 & + \text{Diagram 11} + \text{Diagram 12} - \frac{1}{2} \text{Diagram 13} - \frac{1}{2} \text{Diagram 14}
 \end{aligned}$$

The diagrams represent various loop topologies for the flow equations of the 2-point functions. Diagram 1: A dashed blue circle with two external legs labeled ρ and two internal lines labeled π . Diagram 2: A dashed purple circle with two external legs labeled ρ and two internal lines labeled a_1 . Diagram 3: A dashed blue circle with two external legs labeled ρ and two internal lines labeled a_1 and π . Diagram 4: A solid black circle with two external legs labeled ρ and two internal lines labeled N . Diagram 5: A dashed blue circle with two external legs labeled ρ and two internal lines labeled π . Diagram 6: A dashed blue circle with two external legs labeled a_1 and two internal lines labeled σ and π . Diagram 7: A dashed blue circle with two external legs labeled a_1 and two internal lines labeled π and σ . Diagram 8: A dashed purple circle with two external legs labeled a_1 and two internal lines labeled π and ρ . Diagram 9: A dashed blue circle with two external legs labeled a_1 and two internal lines labeled ρ and π . Diagram 10: A solid black circle with two external legs labeled a_1 and two internal lines labeled N . Diagram 11: A dashed purple circle with two external legs labeled a_1 and two internal lines labeled σ and a_1 . Diagram 12: A dashed blue circle with two external legs labeled a_1 and two internal lines labeled a_1 and σ . Diagram 13: A dashed blue circle with two external legs labeled a_1 and two internal lines labeled π and π . Diagram 14: A dashed blue circle with two external legs labeled a_1 and two internal lines labeled σ and σ .

- ▶ vertices extracted from ansatz for the effective average action Γ_k
- ▶ **aFRG method** allows for **analytic continuation** of flow equations to real energies ω !

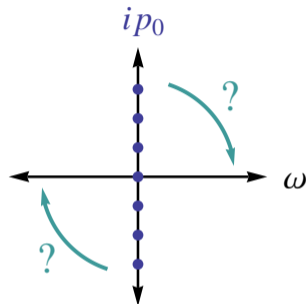
Two-step analytic continuation procedure

1) Use periodicity w.r.t. imaginary energy $ip_0 = i2n\pi T$:

$$n_{B,F}(E + ip_0) \rightarrow n_{B,F}(E)$$

2) Substitute p_0 by continuous real frequency ω :

$$\Gamma^{(2),R}(\omega, \vec{p}) = -\lim_{\epsilon \rightarrow 0} \Gamma^{(2),E}(ip_0 \rightarrow -\omega - i\epsilon, \vec{p})$$



Spectral function is then given by

$$\rho(\omega, \vec{p}) = -\frac{1}{\pi} \text{Im} \frac{1}{\Gamma^{(2),R}(\omega, \vec{p})}$$

[K. Kamikado, N. Strodthoff, L. von Smekal, J. Wambach, Eur.Phys.J. C74 (2014) 2806]

[R.-A. T., N. Strodthoff, L. v. Smekal, and J. Wambach, Phys. Rev. D **89**, 034010 (2014)]

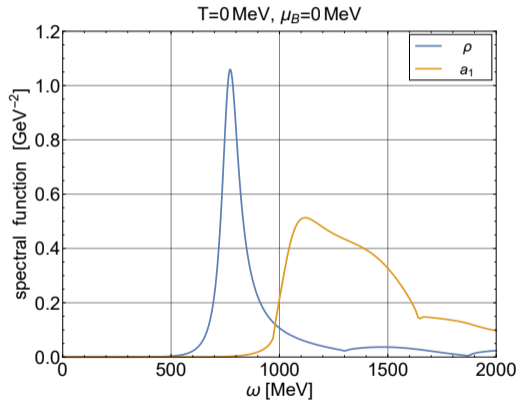
[J. M. Pawłowski, N. Strodthoff, Phys. Rev. D **92**, 094009 (2015)]

[N. Landsman and C. v. Weert, Physics Reports 145, 3&4 (1987) 141]

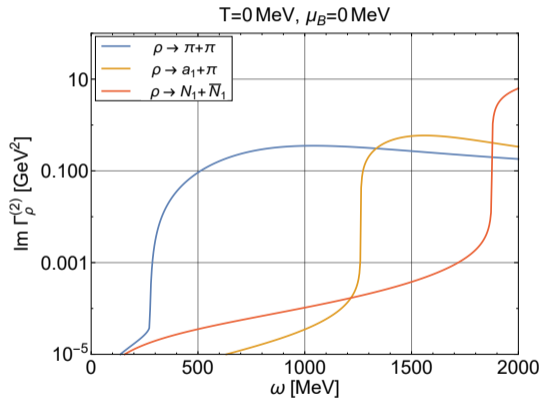
Results on spectral functions and dileptons

ρ and a_1 spectral functions in the vacuum (aFRG)

spectral functions:



imaginary part of ρ 2-point function:

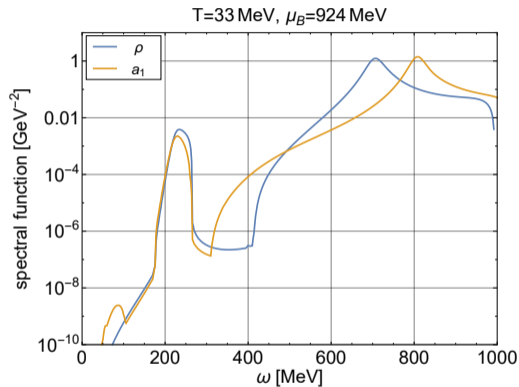


[R.-A. T., C. Jung, L. von Smekal, J. Wambach, Phys. Rev. D 104, 054005 (2021)]

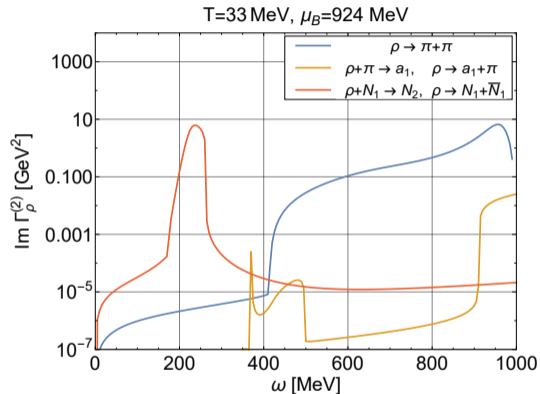
[F. Geurts, R.-A. T., Prog. Part. Nucl. Phys. 128, 104004 (2023)]

ρ and a_1 spectral functions near chiral CEP (aFRG)

spectral functions:

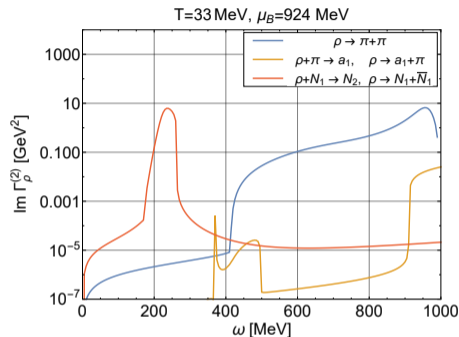
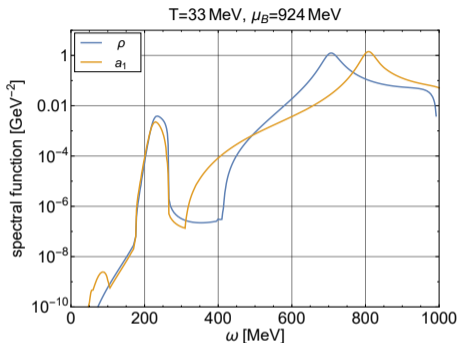


imaginary part of ρ 2-point function:



► a pronounced peak at lower energies due to the process $\rho + N_1 \rightarrow N_2$ is observed!

ρ and a_1 spectral functions near chiral CEP



- peak due to process $\rho + N \rightarrow N^*(1535)$, depends on size of ρ - N - $N^*(1535)$ coupling:

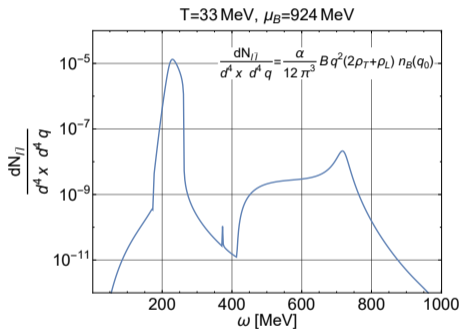
$N(1535)$ BRANCHING RATIOS

$\Gamma(N\rho, S=1/2)/\Gamma_{\text{total}}$				Γ_7/Γ
VALUE (%)	DOCUMENT ID	TECN	COMMENT	
2.7 ± 0.6	ADAMCZEW... 20	DPWA	Multichannel	
14 ± 2	11 HUNT	19 DPWA	Multichannel	

Preliminary results on dilepton rate and spectrum

The resonance-production peak in the ρ spectral function due to the process $\rho + N \rightarrow N^*(1535)$ directly translates into an **enhancement of the thermal dilepton rate**:

dilepton rate from Weldon formula:



[F. Geurts, R.-A. T., Prog. Part. Nucl. Phys. 128, 104004 (2023)]

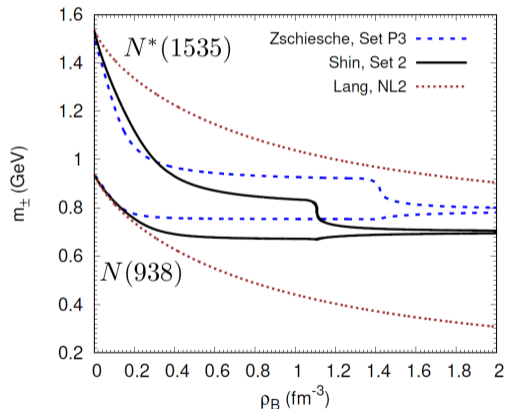
- ▶ unique **prediction of the parity-doublet model!**
- ▶ detection would yield strong evidence in support of the parity-doubling scenario as providing the mechanism for chiral symmetry restoration in dense nuclear matter!

Transport simulation with parity doubling

Parity-doublet model (PDM) mean fields for the nucleon, $N(938)$, and its parity partner, $N^*(1535)$, were included in the GiBUU microscopic transport model:

- ▶ red-dotted line: Walecka mean fields (NL2)
- ▶ black and blue-dashed lines: PDM mean fields (Set 2 and P3)
- ▶ mass of the $N^*(1535)$ resonance decreases quickly with increasing baryon density ρ_B for the PDM fields

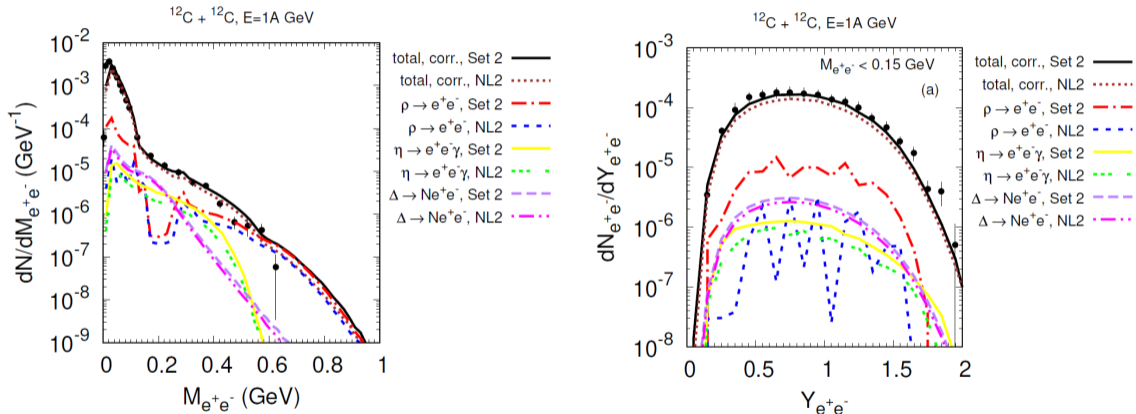
→ **leads to enhancement of $N^*(1535)$ production in the intermediate stages of central heavy-ion collisions at 1 AGeV!**



[A. B. Larionov, L. von Smekal, Phys. Rev. C 105, 034914 (2022)]

Transport simulation with parity doubling

Invariant-mass and rapidity distributions of dileptons in C+C collisions at 1 AGeV with GiBUU:



→ **PDM mean fields lead to enhanced $\rho \rightarrow e^+e^-$ and $\eta \rightarrow e^+e^-\gamma$ signals!**

Summary and Outlook

We computed ρ and a_1 spectral functions in nuclear matter:

- ▶ based on the parity-doublet model and the aFRG method
- ▶ effects of chiral symmetry restoration lead to peak in spectral functions at low energies
- ▶ might be observed experimentally in terms of increased dilepton yield!

Outlook:

- ▶ include repulsive effect ($\sim \omega$) for realistic description of nuclear matter
- ▶ include isospin-chemical potential to describe neutron-rich matter
- ▶ compute equation of state and thermal neutrino rates